# 13.5 Numerical modeling of turbulence above the jet stream during SCATCAT

Todd P. Lane[1]*, James D. Doyle[2], Robert D. Sharman[1], and Melvyn A. Shapiro[3].

[1] *National Center for Atmospheric Research, Boulder CO*
[2] *Naval Research Lab, Monterey CA*
[3] *NOAA / Office of Weather and Air Quality, Boulder CO*

## 1. Introduction

SCATCAT (Severe Clear Air Turbulence Colliding with Aircraft Traffic) 2001 was an experiment, funded by NOAA and the FAA, to examine clear-air turbulence associated with jet streams and upper fronts. NOAA's G-IV aircraft was the principal observing platform, encompassing high resolution dropsonde releases and in-situ measurements. One particular flight, centered around 0Z 18 February 2001, observed an intense jet stream and upper-level frontal structure. While passing over this jet, the aircraft encountered moderate clear-air turbulence.

The 18 February SCATCAT case is the focus of this study. Numerical modeling will be used to examine the details of the jet / front system, and the gravity waves it generates. It will be shown that the gravity waves may be responsible for the turbulence encountered by the G-IV, due to an interaction between these waves and the strong wind shear above the jet.

The observations of the 18 February case will be briefly presented, followed by the results from high-resolution numerical modeling, and finally some conclusions.

## 2. Observations

Surrounding 0Z 18 February 2001, the G-IV released 17 dropsondes (at about 40 km intervals) along a south-west to north-east flight track, which began on the anti-cyclonic side of the jet, passed above the jet core, and finished on the cyclonic side of the jet. The jet core was located at approximately 206°E,40°N. After this flight track, the G-IV completed further passes above the jet core and encountered moderate turbulence, between 33,000 and 37,000 ft.

The dropsonde-derived cross-sections of potential temperature and wind speed are shown in Figs. 1 and 2 respectively. These figures show a strong jet stream with a peak observed wind speed exceeding 100 m/s. Associated with the jet stream is a strong upper-level frontal structure, which is evident in both the potential temperature and wind speed. Above the jet core are strong signatures of vertically propagating gravity waves above about 300 mb (9 km AMSL). These gravity waves have horizontal wavelengths of about 100-150 km. It is in this region of wave activity, above the jet, that turbulence was encountered by the G-IV.

* Corresponding author address: Todd Lane, NCAR, PO BOX 3000, Boulder CO, 80307-3000 USA. E-mail: lane@ucar.edu

For a more detailed analysis of the observations of this case see Koch *et al.* (2003).

## 3. Numerical model calculations

A multi-faceted numerical modeling approach is used, combining a larger-scale forecast model with a small-scale model via a nesting procedure. First, the Coupled Ocean/Atmosphere Mesoscale Prediction System (COAMPS$^{TM}$) completed a 30 hour forecast that is initialized at 0Z 17 February 2001. COAMPS is configured with two domains, the first (second) has 54 km (18 km) horizontal grid spacing, and both domains use the same vertical grid, which has 400 m spacing above the boundary layer. The COAMPS domains are both centered at 203°E, 38°N.

Considering the paucity of observations in the region, the COAMPS forecast compares reasonably well to the observations. The location of the jet is approximately correct in longitude, but about 2 degrees latitude to the north of the observations, and its maximum wind speed is underestimated by about 10 m s$^{-1}$. However, the front becomes best defined after about 3Z 18 February, i.e., a few hours too late. Like the observations, COAMPS produces vertically-propagating gravity waves above the jet core after about 0Z 18 February. The amplitude of these waves increases for the remainder of the forecast.

To examine the details of the jet-front system and the gravity waves it generates in more detail, a cloud-scale model (the Clark model, Clark 1977) is nested within COAMPS. The Clark model is a nonhydrostatic, anelastic model that is capable of two-way interactive grid nesting (Clark and Farley, 1984). The nesting capability allows continued integration of the large-scale flow, while focusing on smaller-scale features.

A number of nested calculations were completed with the Clark model to examine the sensitivity of the modeled flow to changes in grid configuration. These model calculations showed that there is some sensitivity in the solution to grid configuration, due to better modeling of the gradients associated with frontal structures. However, all calculations exhibited similar qualitative structures. In this paper we focus on one of these calculations.

The Clark model simulation to be considered begins at 18Z 17 February 2001, and continues for 12 model hours until 6Z 18 February 2001. The Clark model outermost domain (Domain 1) has 6 km horizontal grid spacing and 400 m vertical grid spacing. The domain is ap-

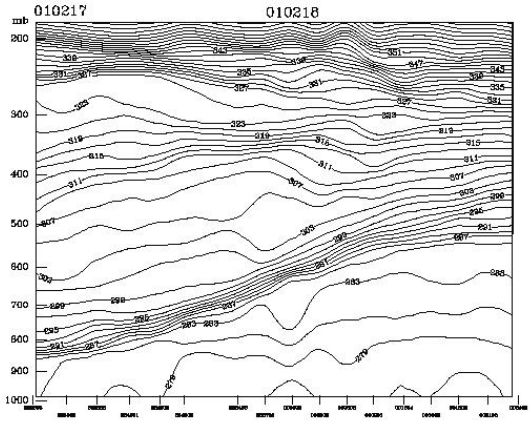


FIG. 1: Contours of potential temperature at 2 K intervals, derived from seventeen dropsondes released around 0Z 18 February 2001. The plot represents two flight legs whose combined horizontal distance is approximately 800 km.

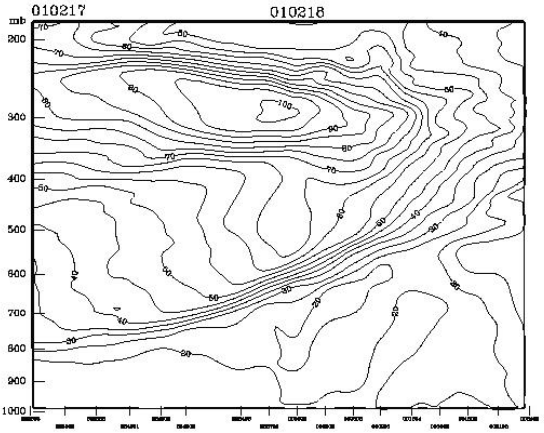


FIG. 2: Same as Fig. 1 except wind speed at 5 m $s^{-1}$ intervals.

proximately 1300 x 1300 km on its lateral boundaries. It extends vertically to 34 km, with the uppermost 10 km featuring a sponge absorber to reduce the reflection of vertical propagating waves off the top boundary. This domain takes its initial conditions from the COAMPS model run, and the boundaries of Domain 1 are forced by the COAMPS data at one-hourly intervals. Two more domains are nested within the Clark model outer domain. The first of these (Domain 2) has 3 km horizontal grid spacing, 200 m vertical grid spacing, is approximately 650 km on each lateral boundary, and extends vertically to approximately 21 km. This domain is initialized from Domain 1 at 0Z, and is integrated until 6Z (18 February 2001). Also initialized at 0Z is Domain 3, which has 3 km horizontal grid spacing, 100 m vertical grid spacing, is approximately 550 km on each lateral boundary, and extends vertically to 14 km. The results from Domain 3 will be the focus of this paper. Note that Domain 2 and Domain 3 have the same horizontal grid spacing but different vertical grid spacings. Domain 2 is only included to provide a more gradual vertical refinement from Domain 1 to Domain 3, which minimizes boundary effects. The center of Domain 3 is at approximately 205°E, 43°N.

Cross-sections, from the south-west to north-east corners of Domain 3, of potential temperature and wind speed at 6Z are shown in Figures 3 and 4 respectively.

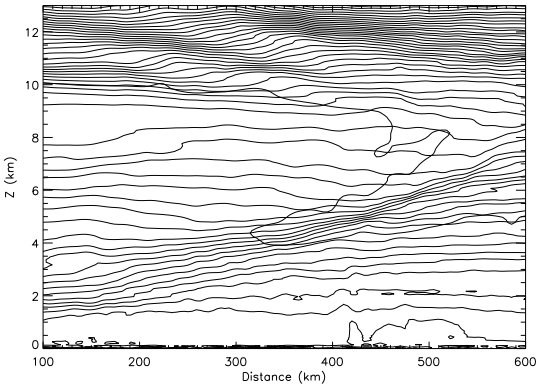


FIG. 3: Contours of potential temperature at 2 K intervals at 6Z 18 February 2001. The cross-section runs from south-west to north-east within Domain 3 of the Clark model. Also shown is the tropopause, defined by 2 PVU potential vorticity contour (thick).

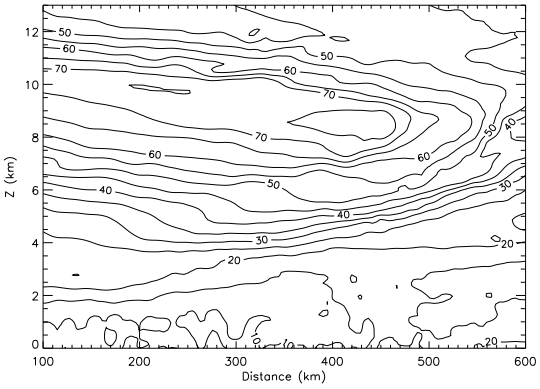


FIG. 4: Same as Fig. 1, except wind speed at 5 m $s^{-1}$ intervals.

This cross-section is in a similar position relative to the jet as the observations, however is at 6Z because this is the time of maximum frontal intensity and gravity wave amplitude in the Clark model. Despite the time delay, there is good qualitative agreement between the modeled flow in the Clark model and that observed. The frontal structure is well represented in the potential temperature field (Figure 3), with strong horizontal gradients. These gradients are larger in the Clark model than that modeled by COAMPS due to the higher vertical and horizontal resolutions. Like COAMPS however, the peak wind speed of

the jet is about 90 m/s. Nonetheless, the vertical wind shear is better represented in the Clark model, particularly above the jet core. Also, there are gravity waves above the jet, shown by perturbations in the potential temperature in the lower stratosphere (10 to 13 km in Figure 3). The location of the gravity waves is in good agreement with the observations. Finally, associated with this jet-front system is a distinct tropopause fold shown by a lowering of the 2 PVU potential vorticity contour (Fig. 3), from its background height of 10 km AMSL down to about 4 km AMSL.

The gravity waves in Fig. 3 are most obvious in the region above the jet / front, from about 2Z to 6Z. This time also corresponds to the maximum frontogenesis, where the horizontal and vertical gradients in potential temperature (from 4 to 8 km AMSL) intensify. Moreover, as the front intensifies the wave amplitude increases. This correlation may suggest that the waves are generated by frontogenesis, however without detailed source analysis it is impossible to make robust conclusions concerning the wave generation mechanism.

The gravity waves evident in Fig. 3 possess a horizontal wavelength of approximately 150 km, and a vertical wavelength of about 2 km. (Given these scales, rotation is probably important and therefore they are inertia gravity waves.) Such a horizontal wavelength is too long to affect aircraft and induce a turbulent response like that experienced by the G-IV. However, as can be seen from close-up views of the potential temperature and wind speed (Figs. 5 and 6) the gravity waves propagating in the lower stratosphere perturb the vertical wind shear and stability. These quantities are perturbed sufficiently that the local Richardson number (Ri) is significantly modified (Fig. 5). In fact, the perturbations in Ri follow the phase lines of the waves, and in regions of upward parcel displacement the Ri is reduced to less than unity and in some regions less then 0.25. Thus, in some regions, the propagating gravity waves have perturbed the flow sufficiently to significantly reduce the Ri, and possibly cause shearing instabilities and turbulence.

The reduced Ri occurs in the negative (speed) shear region above the jet. In this region the magnitude of the shear is large, and consequently the background Ri is small (generally less than 5). [In fact, in both the observations and modeling results the Ri in the upper troposphere and lower stratosphere is (unusually) low over a large region (not shown).] Therefore, in this low Ri region, the relatively small amplitude wave-induced flow perturbations are sufficient to induce possible shearing instability and turbulence.

### 3.1 *A comment on resolution*

When interpreting these model results, one important consideration is whether the results are robust, or unduly affected by grid resolution. Certainly, the waves in the lower stratosphere, with their 150 km horizontal and 2 km vertical wavelengths, are sufficiently resolved with about 30 (20) grid points for each horizontal (vertical)

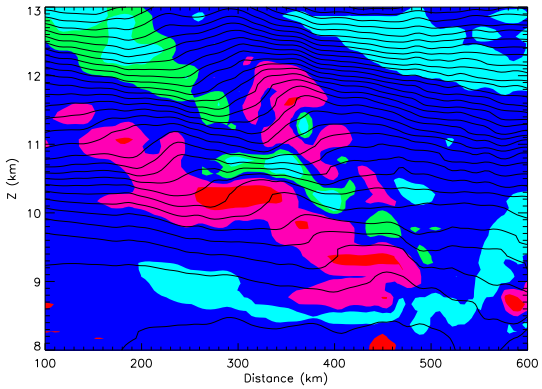


FIG. 5: Same as Fig. 3, except for a smaller area. Also shown is the Richardson number (shaded color) for values less than 0.25 (red), 1 (pink), 2.5 (blue), 5 (green), and greater than 5 (cyan).

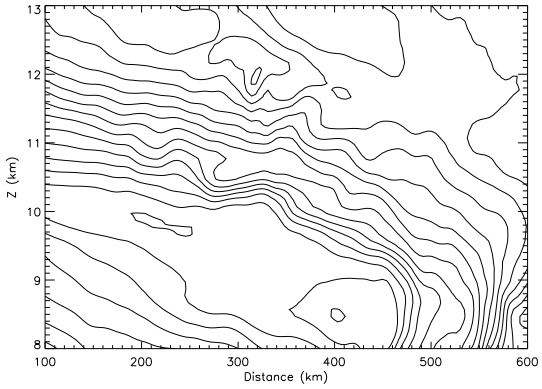


FIG. 6: Same as Fig. 5, except wind speed at 2.5 m $s^{-1}$ intervals.

wavelength. However, are these waves generated by dynamics or numerics? There have been a number of studies that consider this question (e.g., Snyder *et al.* 1993), and it has been shown that a crucial factor is consistent horizontal and vertical resolution. In terms of frontal zones, spurious waves may be generated unless the front is equally well resolved in the horizontal and vertical, i.e., the ratio of vertical to horizontal grid spacing is close to the slope of the front.

In the observations (Fig. 1) and model simulations (Fig. 3), in the south-west to north-east plane, the slope of the front at upper levels is approximately 60:1. While the ratio of horizontal to vertical grid spacing in Domain 3 of the Clark model is 30:1. However, in the horizontal, the frontal zone is oriented at 45 degrees to the model grid (see Fig. 7), and therefore the effective ratio of grid spacings, in the cross-frontal direction, is about 42:1. Therefore, although the effective resolution does not exactly match the slope of the front, it is close and probably sufficient. Also, the gravity waves are relatively insensitive to the resolution, e.g., they exist in a similar form in a simulation with double the grid spacings in both the hor-

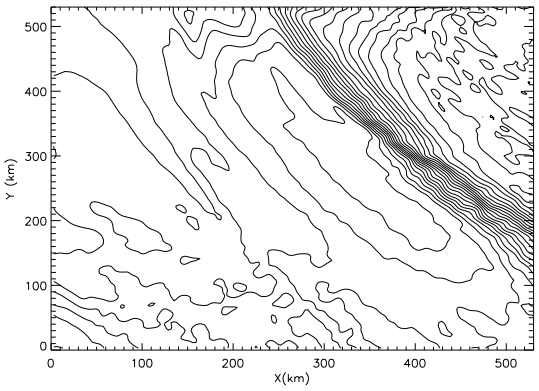


FIG. 7: Horizontal cross-section of potential temperature though 6 km AMSL at 6Z from Domain 3 of the Clark model. The contour interval is 0.5 K.

izontal and vertical. Finally, the modeled gravity waves compare reasonably well with the observations; being in a similar location and having a similar horizontal wavelength. Therefore, the balance of evidence suggests that the gravity waves are dynamically generated and not spurious.

## 4. Summary

In this paper the results from a high-resolution modeling study of the 18 February 2001 SCATCAT case have been presented. This high-resolution simulation showed good agreement with the observations, with a similar jet / front system and similar vertically-propagating gravity waves above the jet core. Above the jet the magnitude of the wind shear was relatively large, and therefore extensive regions of relatively low Ri existed. As the gravity waves propagated through this low Ri region, they perturbed the local shear and stability. Consequently, the gravity waves produced bands of Ri less than 1, and localized regions of Ri less than 0.25. While not explicitly resolved, these wave-induced low Ri regions indicate possible shearing instability and turbulence. Further nesting at higher resolution is planned to better resolve the regions of reduced Ri.

Finally, the results of this study suggest that the coupling between extensive regions of low Ri, and vertically propagating gravity waves generated by frontal zones may be an effective generator of clear-air turbulence. This is a topic of continuing research.

## 5. Acknowledgements

COAMPS$^{TM}$ is a trademark of the Naval Research Laboratory. Figures 1 and 2 were supplied courtesy of NOAA/FSL. This work has benefited from conversations with Steve Koch and Ed Tollerud. We would also like to thank all of the SCATCAT organizers and participants. This research has been funded in part by the Federal Aviation Administration's Aviation Weather Research program. The views expressed are those of the authors and do not represent the official policy or position of the FAA.

## 6. References

Clark, T.L., 1977: A small scale numerical model using a terrain following coordinate transformation. *J. Comput. Phys.*, **24**, 186-215.

Clark, T.L., and R.D. Farley, 1984: Severe downslope windstorm calculations in two and three spatial dimensions using anelastic interactive grid nesting: A possible mechanism for gustiness. *J. Atmos. Sci.*, **41**, 329-350.

Koch, S.E., M.A. Shapiro, B. Jamison, E. Tollerud, and T. Smith, 2003: Generation of turbulence within an upper-tropospheric front. *Proc. 10th Conf. on Mesoscale Processes*, Portland OR, P2.24.

Snyder, C., W. C. Skamarock, and R. Rotunno, 1993: Frontal dynamics near and following frontal collapse. *J. Atmos. Sci.*, **50**, 3194-3211.